Nicastrin modulates presenilin-mediated *notch/glp-1* signal transduction and βAPP processing

Gang Yu*†, Masaki Nishimura*†, Shigeki Arawaka*, Diane Levitan‡, Lili Zhang‡, Anurag Tandon*, You-Qiang Song*, Ekaterina Rogaeva*, Fusheng Chen*, Toshitaka Kawarai*, Agnes Supala*, Lyne Levesque*, Haung Yu*, Dun-Sheng Yang*, Erin Holmes*, Paul Milman*, Yan Liang*, Dong Mei Zhang*, Dong Hong Xu*, Christine Sato*, Evgeny Rogaev*, Marsha Smith‡, Christopher Janus*, Yanni Zhang§, Ruedi Aebersold§, Lindsay Farrer‖, Sandro Sorbi¶, Amalia Bruni#, Paul Fraser* & Peter St George-Hyslop*

** Centre for Research in Neurodegenerative Diseases; The University Health Network (Toronto Western Hospital); and Departments of Medicine (Neurology) and Medical Biophysics, University of Toronto, Tanz Neuroscience Building, 6 Queen's Park Crescent West, Toronto, Ontario, M5S 3H2, Canada*
‡ Department of CNS and Cardiovascular Research, Schering Plough Research Institute, 2015 Galloping Hill Road, Kenilworth, New Jersey 07033-0539, USA
§ Molecular Biotechnology, University of Washington, Seattle, Washington 98195-7730, USA
‖ Genetics Program, Boston University School of Medicine, 80 East Concord Street, Boston, Massachusetts 02118-2394, USA
¶ Department of Neurology, University of Florence, viale Morgagni 65, Florence 50134, Italy
 # Centro Regionale di Neurogenetica, USL 6, Lamezia Terme 88046, Italy
† These authors contributed equally to this work

Nicastrin, a transmembrane glycoprotein, forms high molecular weight complexes with presenilin 1 and presenilin 2. Suppression of nicastrin expression in *Caenorhabditis elegans* embryos induces a subset of *notch/glp-1* phenotypes similar to those induced by simultaneous null mutations in both presenilin homologues of *C. elegans* (*sel-12* and *hop-1*). Nicastrin also binds carboxy-terminal derivatives of β-amyloid precursor protein (βAPP), and modulates the production of the amyloid β-peptide (Aβ) from these derivatives. Missense mutations in a conserved hydrophilic domain of nicastrin increase $Aβ_{42}$ and $Aβ_{40}$ peptide secretion. Deletions in this domain inhibit Aβ production. Nicastrin and presenilins are therefore likely to be functional components of a multimeric complex necessary for the intramembranous proteolysis of proteins such as Notch/GLP-1 and βAPP.

Presenilin 1 (PS1)[1] and presenilin 2 (PS2)[2] are conserved, polytopic transmembrane proteins that are functional components of separate high molecular weight complexes[3,4] resident in the endoplasmic reticulum (ER) and Golgi apparatus[5]. PS1 and PS2 are essential for an unusual, but poorly understood form of proteolytic cleavage that occurs within the transmembrane domains of several proteins, including βAPP[6], Notch[7–10] and Ire1p[11,12]. In addition, the intramembranous proteolysis of βAPP (termed γ-secretase cleavage) is increased by missense mutations in the presenilins associated with familial Alzheimer's disease (FAD)[1,2], resulting in overproduction of the neurotoxic Aβ derivative[13,14]. Evidence suggests that the presenilins may have direct catalytic activity[15,16]; however, three observations indicate that this activity requires at least interactions between the presenilins and other proteins. First, the abundance of PS1 and PS2 is tightly regulated by the limited abundance of another unknown component of the presenilin complexes[17]. Second, PS1 co-fractionates with γ-secretase enzymatic activity in a very high molecular weight complex[18]. Third, loss-of-function mutations in two intramembranous aspartate residues[15] alter the structure and size of the presenilin complexes[19], suggesting that these aspartate residues also affect critical interactions between the presenilins and other components of these complexes.

Here we report the identification of a new component of PS1 and PS2 complexes. This component, nicastrin, is a Type I transmembrane glycoprotein which interacts with both PS1 and PS2, and which has a central role in presenilin-mediated processing of βAPP and some aspects of *notch/glp-1* signalling *in vivo*. The name nicastrin reflects the fact that the quest for the molecular machinery causing the presenilin-associated forms of Alzheimer's disease began nearly 40 years ago with the description of Alzheimer's disease in descendants of an extended family originating in the Italian village of Nicastro[20,21].

Isolation of nicastrin

HEK293 cells physiologically process βAPP to Aβ peptide, contain β-secretase and display the same biochemical effects of mutations in Alzheimer's disease genes (βAPP, PS1 and PS2) as observed *in vivo* in human and murine brain. We therefore used an anti-PS1 antibody (Ab1142 to residues 30–45) to immuno-extract PS1 and tightly associated proteins from intracellular membrane fractions of HEK293 cells expressing moderate levels of PS1. Coomassie-blue-stained SDS–polyacrylamide gel electrophoresis (PAGE) gels of the immuno-purified proteins contained two intense bands in addition to those of the PS1 holoprotein and its fragments (see Supplementary Information). Solid phase microextraction-capillary zone electrophoresis-microelectrospray (SPE-CE) tandem mass spectroscopy[22] identified the proteins in these bands as a new protein (nicastrin), and α- and β-catenin. Catenins have previously been shown to interact with presenilins[3,4,23,24].

The deduced amino-acid sequence of the nicastrin peptide was identical to that predicted for several anonymous partial complementary DNAs in public databases. The partial cDNAs were used to derive a full-length nicastrin cDNA (GenBank Accession number AF240468). The human *nicastrin* gene maps to a region of chromosome 1 (near *D1S1595* and *D1S2844*) that, in two independent genome-wide surveys[25,26], has generated evidence for genetic linkage and/or allelic association with an Alzheimer's disease susceptibility locus. The *nicastrin* gene encodes an open reading frame of 709 amino acids containing a putative amino-terminal signal peptide; a long N-terminal hydrophilic domain containing glycosylation, *N*-myristoylation and phosphorylation motifs; a ~20-residue hydrophobic putative transmembrane domain; and a short hydrophilic carboxy terminus of 20 residues (Fig. 1). However, we could not find any significant amino-acid sequence homology or strong motif similarity to other functionally characterized proteins.

In the absence of homology to other proteins, we screened sequence databases for orthologous genes in other species. We found a full-length *C. elegans* nicastrin orthologue (ZC434.6) in public databases (accession no. Q23316; $P = 1e^{-37}$; identity = 22%; similarity = 41%). We cloned and sequenced full-length murine and *Drosophila* nicastrin orthologues from appropriate cDNA libraries using partial cDNA sequences from these databases as start points (mouse nicastrin accession no. AF24069, $P = 0.00$, identity = 89%, similarity = 93%; *D. melanogaster* nicastrin accession no. AF240470, $P = 4e^{-77}$, identity = 30%, similarity = 48%). A weakly similar protein is also predicted to exist in the plant *Arabidopsis* (accession no. CAB89225.1, $P = 8e^{-22}$, identity = 26%, similarity = 40%). The four animal nicastrins have similar predicted topologies and have three domains with significant sequence conservation near residues 306–360, 419–458, and 625–662 of human nicastrin ($P < 1e^{-06}$; identities = 50–89%, similarities = 60–90% for each segment) (Fig. 1). Within the first conserved domain, all four proteins contained the motif DYIGS (residues 336–340), which is also partially conserved in the *Arabidopsis* protein. All four animal nicastrins also contain four cysteines spaced at 16–17-residue intervals in the N terminus (Cys 195, Cys 213, Cys 230 and Cys 248).

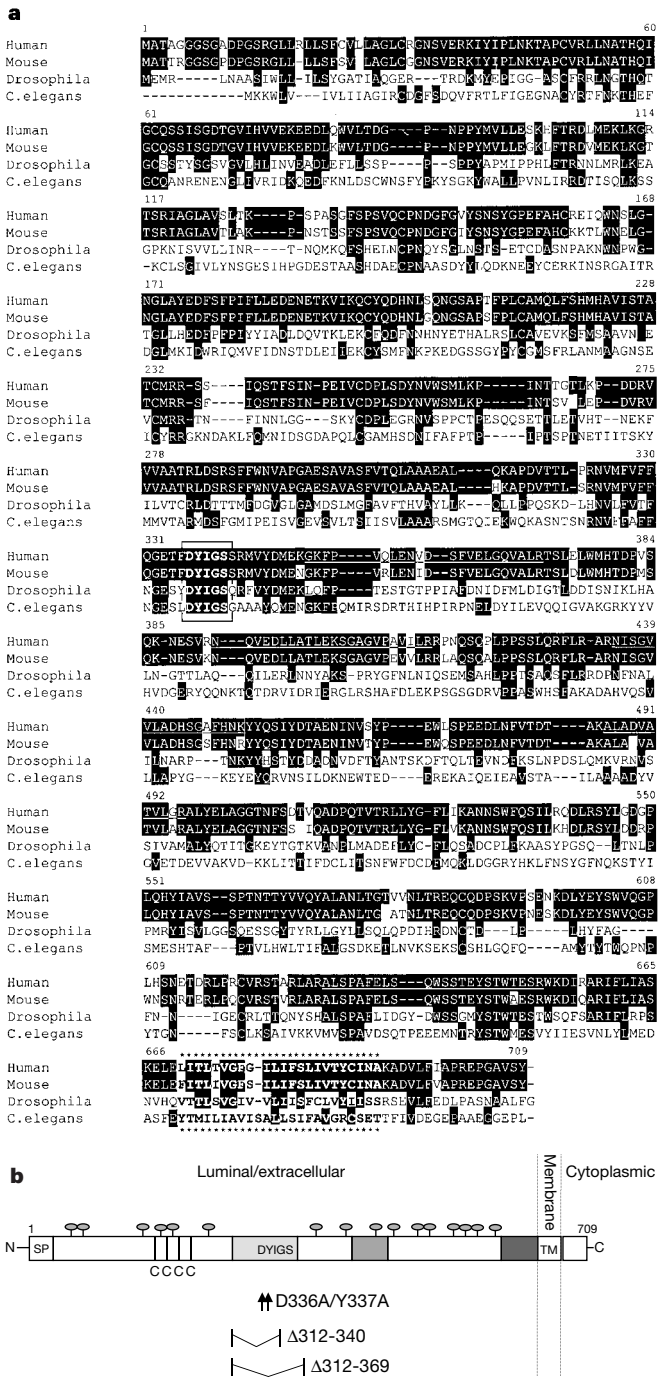

Figure 1 Predicted amino-acid sequence and topology of nicastrin. **a**, Predicted sequence of human nicastrin and murine, *D. melanogaster* and *C. elegans* nicastrin orthologues. Asterisks denote a putative transmembrane domain. Peptide fragments identified by mass spectroscopy are underlined. Conserved sequences are highlighted. The DYIGS motif is boxed. **b**, Predicted topology of human, murine, *D. melanogaster* and *C. elegans* nicastrin orthologues. SP, signal peptide; C, four conserved cysteines; ovals, potential glycosylation sites; TM, transmembrane domain. Shading indicates highly conserved domains. The location of the DYIGS motif and functionally active missense (arrows) and deletion mutations (between vertical lines) are shown.

Nicastrin interacts with presenilins

Western blots of lysates from HEK293 cells transfected with a V5-epitope-tagged nicastrin cDNA revealed a V5-immunoreactive band with a relative molecular mass of about 110,000 ($M_r \approx$ 110K). Following digestion by Endo H, this band was reduced to ~80K (the predicted size of the nicastrin amino-acid sequence), confirming that nicastrin is glycosylated (Fig. 2, lanes 1–4). The V5-immunoreactive band was also detected by the anti-nicastrin antibodies anti-N-NCT (against human nicastrin residues 290–406) and anti-C-NCT (against residues 691–709) (Fig. 2, lane 5). In cells transiently transfected with V5–nicastrin, a series of M_r ~ 7K–10K fragments were observed which we predict contain the transmembrane domain and short C terminus of nicastrin plus the V5 epitope of M_r 3K (Fig. 2, lane 1). However, because they are not detectable in stably transfected cells (Fig. 2, lane 3) and no secreted N-terminal fragments were detected in conditioned media, it is unclear whether or not these C-terminal derivatives are artefacts of over-expression.

Immunoprecipitation studies in human brain (Fig. 3a) and in transfected HEK293 cells (see Supplementary Information) confirm

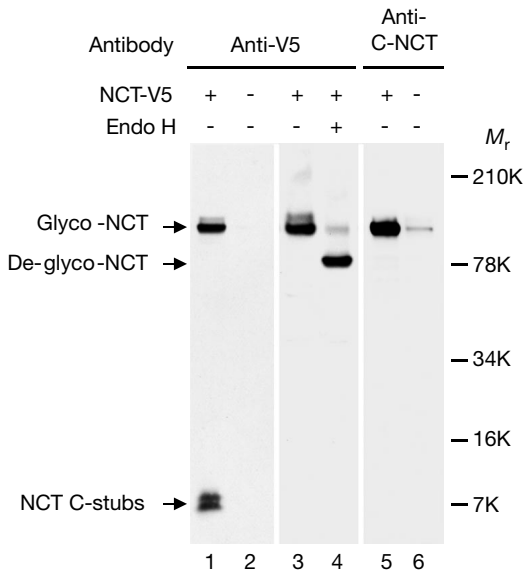

Figure 2 Characterization of nicastrin (NCT) using V5-tagged nicastrin. Immunoblots of lysates from HEK293 cells either transiently transfected (lane 1) or stably transfected with NCT–V5 (lanes 3–5) probed with anti-V5 antibody (lanes 1–4) or with a C-terminal anti-NCT antibody (anti-C-NCT, lanes 5–6). In transiently transfected cells, C-terminal stubs of nicastrin can be detected, which are not present in stable cell lines. Endo H treatment shows nicastrin is glycosylated (lane 4). The anti-C-NCT antibody (lane 5) detects the same band as the anti-V5 antibody in NCT–V5 stably transfected cells, and also detects a small amount of endogenous nicastrin in untransfected cells (lane 6).

that the nicastrin–PS1 interaction is authentic and specific ($n > 4$ replications). Thus, pre-immune serum, antibodies to other proteins resident in the endoplasmic reticulum (for example, calnexin), and other V5-tagged proteins (in studies using HEK293 cells) do not co-precipitate either nicastrin or PS1. Glycerol velocity centrifugation gradients showed that nicastrin co-fractionates with the high molecular weight PS1 and PS2 complexes. Nicastrin and PS1 strongly co-localize with markers of the endoplasmic reticulum and Golgi in MDCK cells, and their patterns of transcription overlap on northern blots from human tissues (see Supplementary Informtaion). Parallel studies confirmed that nicastrin also interacts with PS2 in human brain (Fig. 3a) and in HEK293 cells (see Supplementary Information). Finally, co-immunoprecipitation experiments revealed that nicastrin interacts equivalently with wild-type PS1, with PS1-L392V (an FAD-related gain-of-function mutant that increases Aβ secretion[1,14]) and with PS1-D385A (a loss-of-function mutant that inhibits γ-secretase and Aβ secretion[15]) (n = 3 replications, Fig. 3b).

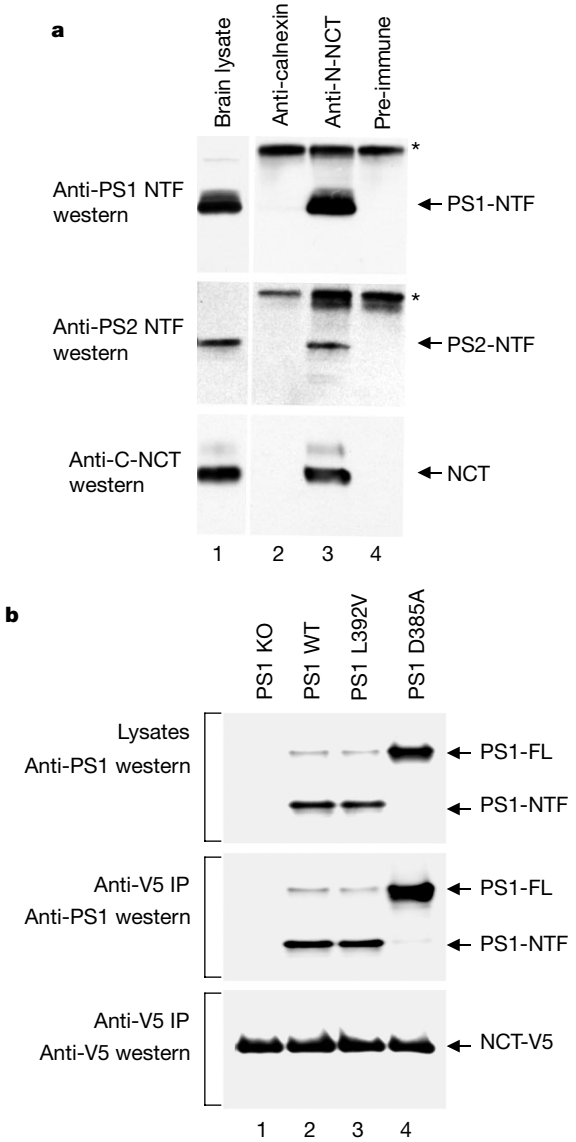

Figure 3 PS1 and PS2 form complexes with nicastrin. **a**, In digitonin-solubilized human brain lysates, antibody to the N terminus of nicastrin (anti-N-NCT; lane 3) co-precipitates endogenous PS1 (top panel), PS2 (middle panel) and nicastrin itself (bottom panel). Antibodies to calnexin (lane 2) and pre-immune serum (lane 4) do not co-precipitate PS1, PS2 or nicastrin. Asterisk corresponds to immunoglobulin. The column labelled 'brain lysate' (lane 1) contains about 25% of the starting lysate used for immunoprecipitation. **b**, Nicastrin interacts equivalently with mutant and wild-type PS1. Anti-V5 immunoprecipitation products from NCT–V5 transiently transfected embryonic fibroblasts from PS1-knockout mice or from wild-type mice stably overexpressing human wild-type PS1 (PS1-WT), PS1-L392V or PS1-D385A were investigated for PS1 with anti-PS1 antibody 14.3 (middle panel), or for NCT–V5 (bottom panel). Western blot of the starting lysates (top panel) shows the initial amounts of PS1.

Nicastrin and *notch* signalling

To explore whether nicastrin, like the presenilins, might have a role in *notch* signalling *in vivo*, we used RNA interference (RNAi) in *C. elegans*. Wild-type worms injected with *C. elegans* nicastrin double-stranded (ds) RNA produced dead embryos, many of which lacked an anterior pharynx (Fig. 4, bottom panel). This phenotype was highly reproducible ($n > 35$ animals injected in 5 replications) and specific (the phenotype was not observed with injection buffer or with ~50 unrelated double stranded RNAs). Except for embryonic lethality, none of the other phenotypes associated with a lack of *C. elegans* presenilin (*sel-12*) activity were observed. However, this phenotype is identical to that induced when the activity of genes in the *notch/glp-1* pathway (*glp-1*, *aph-1* or *aph-2*) are reduced, or when the activities of both *C. elegans* presenilin homologues (*sel-12* and *hop-1*) are reduced simultaneously[27–29]. Subsequently, we learned that *aph-2* has been mapped to a spontaneous transposon insertion mutant in the ZC434.6 gene[30], confirming that *aph-2* and nicastrin are identical and that nicastrin contributes to some aspects of *notch/glp-1* signalling in *C. elegans* embryos.

Nicastrin modulates γ-secretase cleavage of βAPP

The βAPP holoprotein (FL-βAPP) is physiologically processed by a two-step proteolytic pathway. Initially, FL-βAPP is cleaved near the cell surface in its extracellular domain either by β-secretase (to generate a membrane-bound 99-residue C-terminal stub, C99-βAPP)[31–34], or by a putative α-secretase (to generate an 83-residue membrane-bound C-terminal stub, C83-βAPP). These stubs are then further cleaved within their transmembrane domains by the presenilin-linked γ-secretase to generate Aβ and p3 respectively. The γ-site cleavage can occur at either of two positions to form

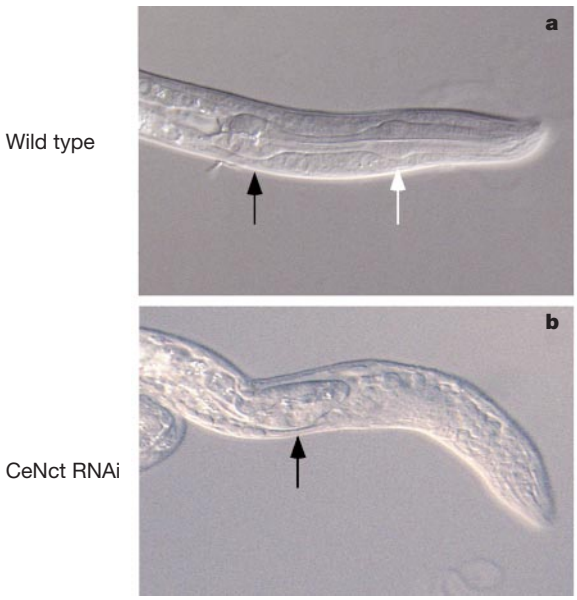

Figure 4 Effect of nicastrin on Notch signalling. Black arrow points to the posterior bulb of the pharynx; white arrow points to anterior bulb of the pharynx. **a**, Newly hatched non-injected L1 animal. **b**, Newly hatched L1 animal after dsRNA injection into a wild-type parent. Note the complete absence of the anterior bulb of the pharynx in nicastrin RNAi-treated *C.elegans* embryos.

$A\beta_{40}$ (predominant isoform) or $A\beta_{42}$ (fibrillogenic, neurotoxic isoform)[35].

To assess the role of nicastrin–presenilin complexes in βAPP processing, we investigated anti-nicastrin co-immunoprecipitation products to determine whether nicastrin might directly interact with βAPP and/or its C-terminal derivatives. An antibody to the C terminus of βAPP (Ab369) detected both FL-βAPP and C99-βAPP/C83-βAPP in the anti-nicastrin co-immunoprecipitation products from digitonin lysates of HEK293 cell lines stably expressing wild-type βAPP (n = 4 replications, Fig. 5a). This was confirmed in HEK293 cells over-expressing either $\beta APP_{Swedish}$ or the SpC99-βAPP cDNA (encoding the signal peptide and C-terminal 99 residues of βAPP) ($n > 4$ replications, Fig. 5b). In Fig. 5b, nicastrin appears to interact better with C99-βAPP than with C83-βAPP; however, C83-βAPP is less abundant in these cells (Fig. 5b, lanes 1–4). In fact, nicastrin interacts with both C99-βAPP and C83-βAPP stubs (Fig. 5c, lane 9). Of greater interest, the genotype of the co-expressed PS1/PS2 molecule dynamically influenced the interaction of nicastrin with C99-βAPP/C83-βAPP. After transient transfection of nicastrin, more C99-βAPP/C83-βAPP stubs co-immunoprecipitated with nicastrin in cells expressing the FAD-associated PS1-L392V mutation than in cells expressing wild-type PS1 (and equivalent quantities of nicastrin and C99-βAPP) (n = 4 replications, Fig. 5b, lanes 2 and 4). Conversely, much less C99-βAPP/C83-βAPP stubs co-immunoprecipitated with nicastrin in cell lines expressing the loss-of-function PS1-D385A mutation (despite the presence of very large amounts of C-terminal βAPP derivatives in these cells) (n = 4 replications, Fig. 5b, lanes 2 and 6).

Similar, but less robust effects were also observed in cells over-expressing full-length $\beta APP_{Swedish}$ plus PS2 (wild-type, FAD PS2-N141I or loss-of-function PS2-D366A mutants) (Fig. 5b, lanes 9–11). More notably, the PS1-sequence-related differences in the nicastrin–C99-βAPP/C83-βAPP interaction were most evident within 24 h of transfection with nicastrin (Fig. 5b, c). By 72 h, the amount of C99-βAPP/C83-βAPP that immunoprecipitated with nicastrin reached a new equilibrium, and was roughly equivalent in cells expressing different PS1-sequences (n = 2 replications, Fig. 5c). This dynamic change was not due to changes in the levels of PS1, C-terminal βAPP derivatives (data not shown) or nicastrin (Fig. 5c). One interpretation is that the presenilins may be

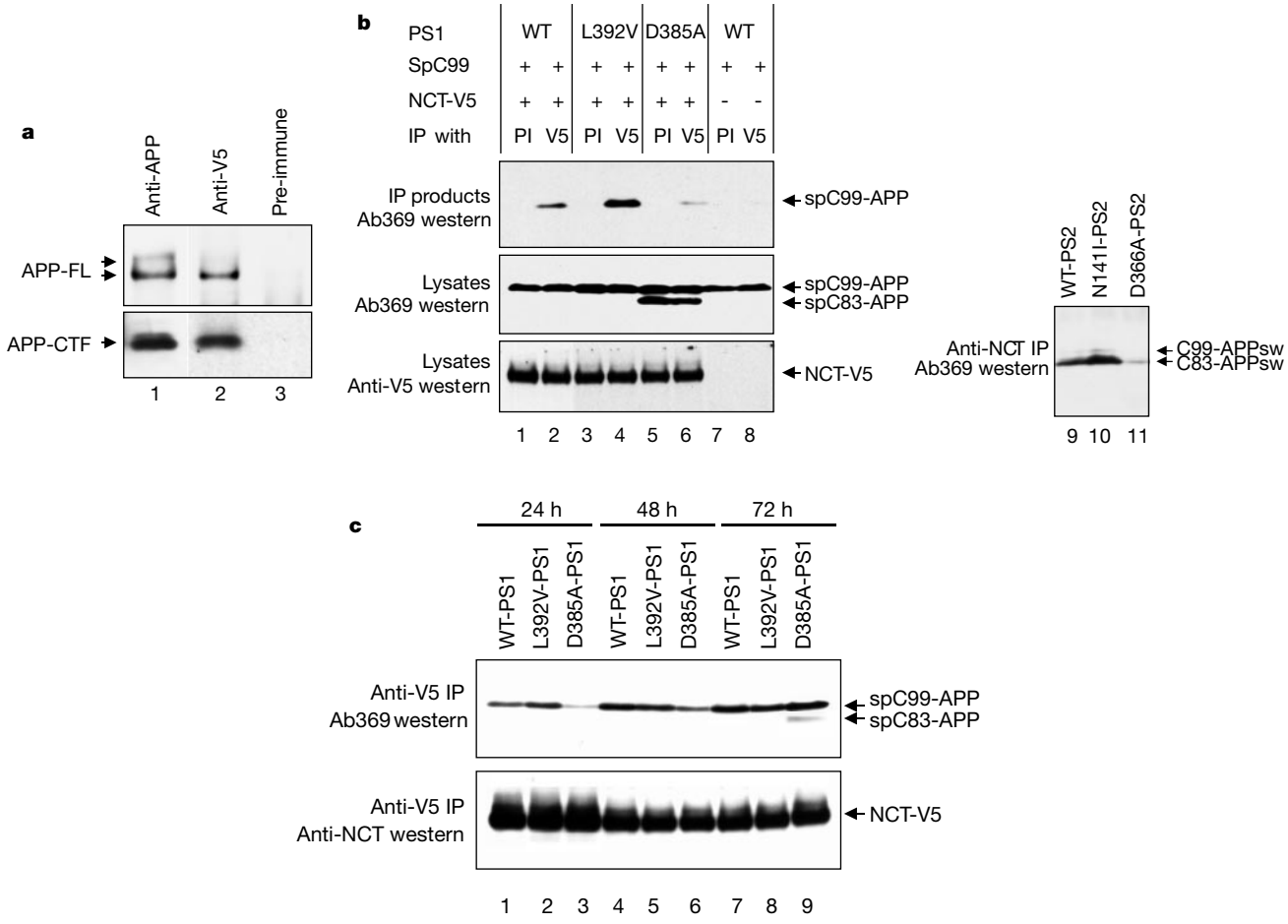

Figure 5 α-secretase and β-secretase cleavage fragments of βAPP (C83-βAPP and C99-βAPP respectively) co-precipitate with nicastrin. **a**, Western blot of anti-NCT–V5 immuno-precipitates from HEK293 cells expressing nicastrin and wild-type βAPP reveals FL-βAPP and C99-βAPP/C83-βAPP (detected with antibody 369; lane 2). FL-βAPP and C99-βAPP/C83-βAPP do not co-precipitate with pre-immune serum (lane 3). Note, for anti-APP (lane 1), about 10% of the starting lysate was used for immunoprecipitation. **b**, Top left, HEK293 cells stably expressing the SpC99-βAPP construct together with either wild-type PS1 (WT-PS1), L392V-PS1 or D385A-PS1 were transiently transfected with NCT–V5 for 24 h. The NCT–V5 immunoprecipitation products ('V5' lanes) but not the pre-immune immunoprecipitation products (PI) contain C99-βAPP fragments (detected with antibody 369 to C terminus of βAPP). Middle left, anti-C-terminus of βAPP immunoblot of the same lysates (antibody 369) showing starting levels of C99-βAPP/C83-βAPP (increased amounts of C83-βAPP in lanes 5 and 6 reflect inhibition of γ-secretase cleavage of C83-βAPP by the D385A-PS1 mutant). Bottom left, anti-V5 immunoblot of the same lysates showing similar starting levels of NCT–V5. Bottom right, identical results were obtained with cells stably expressing PS2 (wild type, N141I, D366A) and full-length APP (APP_{sw}), and transiently transfected with untagged nicastrin for 24 h. **c**, In the same HEK293 lines, the genotype at PS1 dynamically influences the amount of βAPP stubs co-immunoprecipitating with nicastrin. The differences are most marked 24 h after transient transfection of nicastrin, and reach a new higher, steady state at 72 h. Note that the D385A-PS1 cells have higher basal levels of C99-βAPP and C83-βAPP fragments compared with wild-type cells.

dynamically involved in regulating or loading nicastrin with the substrates of γ-secretase.

To explore the role of nicastrin in Aβ production, we created a series of HEK293 cell lines stably overexpressing $\beta APP_{Swedish}$ plus either wild-type or mutant nicastrin. Relative to mock-transfected or LacZ-transfected cells, overexpression of wild-type and most mutant nicastrins had no significant effect on Aβ secretion. However, missense mutation of the conserved DYIGS motif to AAIGS (residues 336–340) caused a significant increase in Aβ secretion, and especially in $Aβ_{42}$ secretion ($P < 0.001$, Fig. 6; 5 independent clonal cell lines, 29 total observations). Conversely, deletion of the DYIGS domain in two independent constructs (NCTΔ312–369 and NCTΔ312–340) caused a significant reduction in both $Aβ_{42}$ and $Aβ_{40}$ secretion. This was more profound in NCTΔ312–369 cells than in NCTΔ312–340 cells (Fig. 6, five independent clones in total). These effects are similar to the effects of gain-of-function and loss-of-function mutations in the presenilins, respectively. However, in contrast to $PS1^{-/-}$ and PS1-D385A mutants, the reduction in Aβ secretion induced by the NCTΔ312–369 and NCTΔ312–340 mutants was not accompanied by accumulation of C99-βAPP and C83-βAPP stubs. This suggests that C99-βAPP and C83-βAPP stubs that do not enter the nicastrin–presenilin complex for γ-secretase cleavage are degraded by other pathways.

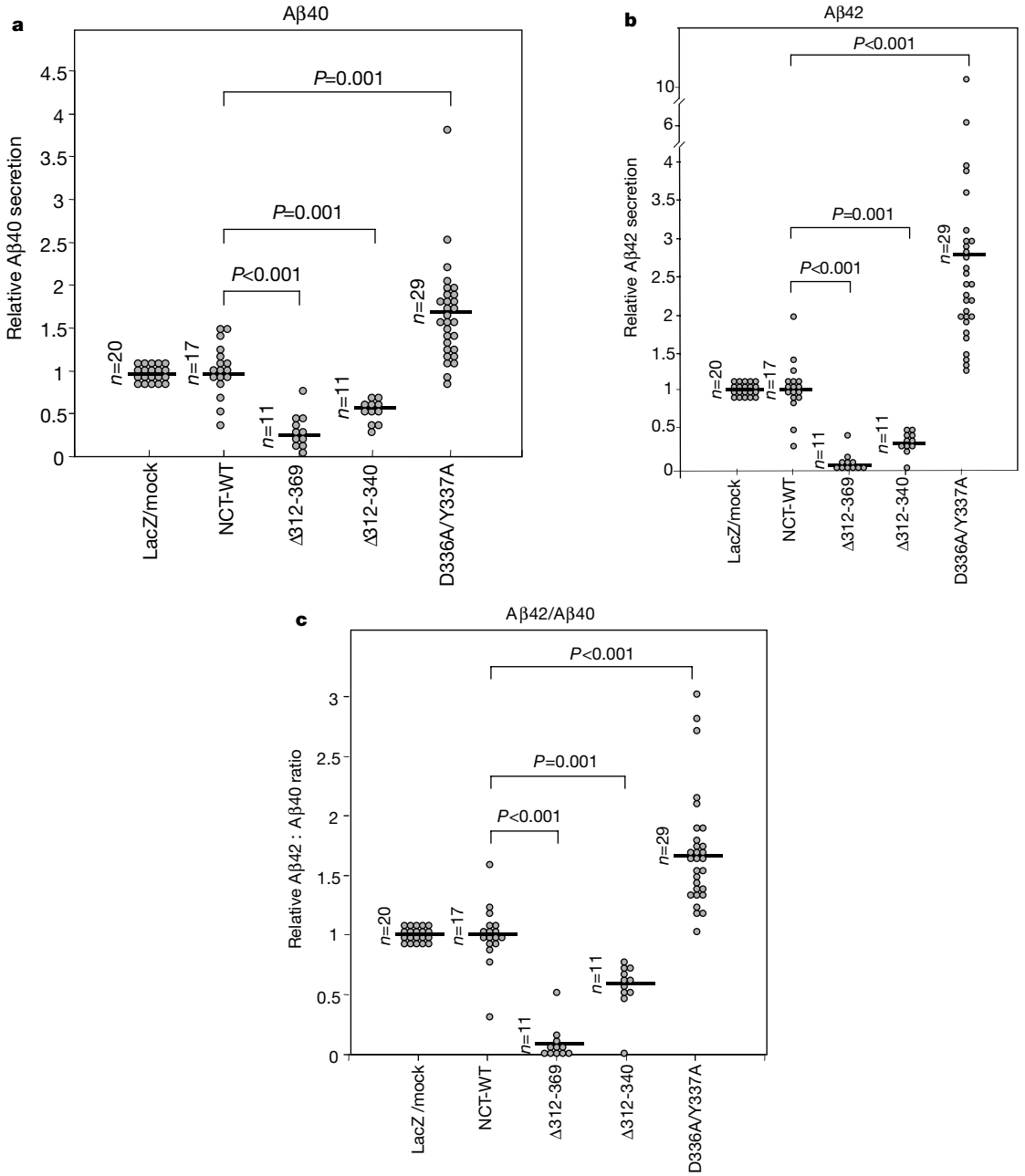

Figure 6 Scatter plots of secreted $Aβ_{40}$, $Aβ_{42}$ and $Aβ_{42}/Aβ_{40}$ ratios showing increased Aβ secretion from HEK293 cells expressing DYIGS→AAIGS mutant nicastrin, and decreased Aβ secretion from cells expressing Δ312–369 or Δ312–340 mutants. Each dot represents a single experiment performed on LacZ/mock transfected controls expressing APP_{sw} (lane 1, 3 independent cell lines); wild-type nicastrin plus APP_{sw} (lane 2, 5 cell lines); Δ312–369 NCT plus APP_{sw} (lane 3, 2 cell lines); Δ312–340 NCT plus APP_{sw} (lane 4, 3 cell lines); DYIGS→AAIGS NCT plus APP_{sw} (lane 5, 5 cell lines). The Aβ level in mock-transfected or LacZ-transfected control samples was normalized to 1.0. Aβ levels in test samples were expressed relative to this normalized value. Mean normalized values are depicted by horizontal bar (see Supplementary Information). *P* values represent comparisons of normalized Aβ levels from media of cells expressing mutant nicastrin relative to levels from cells expressing wild-type nicastrin.

The effects of nicastrin mutations on Aβ secretion are not due to trivial explanations such as differences in the levels of nicastrin, βAPP holoprotein or PS1/PS2, nor are they due to effects on the activity of α- or β-secretase (see Supplementary Information). None of the mutations affect the interaction of nicastrin with C99-/C83-βAPP (Fig. 7). However, although the DYIGS→AAIGS mutant of nicastrin can efficiently co-immunoprecipitate PS1, both of the deletion mutants significantly reduced the nicastrin–PS1 interaction (Fig. 7, two independent cell lines each, in triplicate). Furthermore, the magnitude of this effect was proportional to the effect of each of the deletion mutants on Aβ secretion (Fig. 7). Residues 312–369 of nicastrin contain no obvious functional motifs or sequence homology to other known proteins. Consequently, mutations in this domain presumably either affect a presenilin-binding domain, or they affect a regulatory domain that modulates both the nicastrin–PS1 interaction and the subsequent γ-secretase-mediated cleavage of nicastrin-bound C99-βAPP and C83-βAPP stubs.

Conclusions

Our data indicate that nicastrin is an authentic, functional component of PS1 and PS2 complexes. Nicastrin is unlikely to be simply another Type I membrane protein whose processing involves the presenilins (for example, like βAPP). First, nicastrin is a principal stoichiometric component of the presenilin complexes. In contrast, substrates like βAPP and Notch are not principal constituents of the high molecular weight presenilin complexes, and can only be inconsistently co-precipitated with PS1/PS2 (refs 3, 36–39). Second, the role of nicastrin in the presenilin-mediated processing of both βAPP and Notch would not be expected if nicastrin were simply another substrate.

These results suggest that nicastrin is part of a new functional complex (putatively a 'secretasome') involved in the unusual intramembranous proteolytic processing of transmembrane proteins like βAPP and Notch. The exact role of nicastrin is currently unclear. Although the primary amino-acid sequence of nicastrin does not resemble known proteases, we cannot entirely exclude a proteolytic function. However, the current data are compatible with two other models. One model for nicastrin activity is a role in binding the substrates of the presenilin–γ-secretase complexes (and/or other γ-secretase-like enzymes). Our data suggest that this binding is dynamically modulated by presenilin mutations in a direction commensurate with the effect of each particular presenilin mutation on γ-secretase activity. Thus, presenilin FAD-mutations increase nicastrin binding to C99-βAPP/C83-βAPP and increase Aβ secretion whereas presenilin aspartate mutants have the opposite effect.

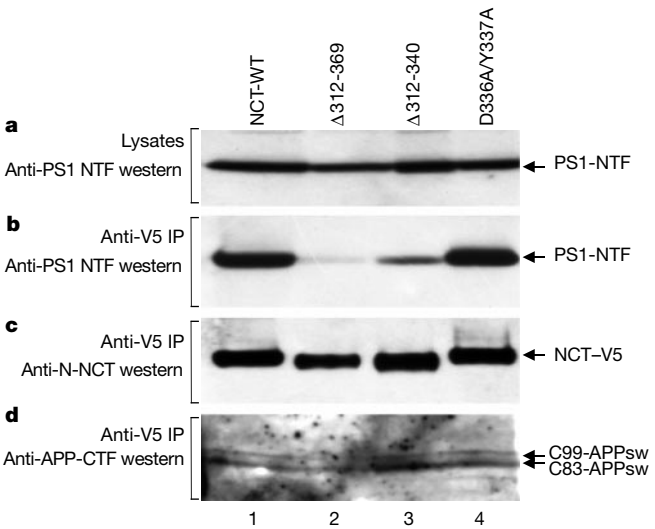

Figure 7 Functional nicastrin mutants do not significantly impair the nicastrin interaction with C99-βAPP/C83-βAPP in HEK293 cells expressing $βAPP_{Swedish}$. The DYIGS→AAIG mutant of NCT has no discernible effect on the NCT–PS1 interaction, but the NCTΔ312–369 or NCTΔ312–340 mutations do impair the NCT–PS1 interaction proportional to their effect on Aβ secretion. **a**, Lysates probed with anti-PS1-NTF antibody (Ab14). **b**, Anti-V5 NCT immunoprecipitation products probed with anti-PS1-NTF antibody (Ab14). **c**, Anti-V5 NCT immunoprecipitation products probed with anti-NCT antibody (anti-N-NCT). **d**, Anti-V5 NCT immunoprecipitation products probed with anti-C-terminal βAPP antibody 369. Note, a longer exposure was used for this immunoblot.

Whether or not genetic variants in nicastrin are associated with inherited susceptibility to Alzheimer's disease remains to be seen. In preliminary studies, we have found no mutations or polymorphisms in the open reading frame of nicastrin in affected members of 19 late onset FAD pedigrees in which no obligate recombinants were detected between Alzheimer's disease and the *D1S1595*–14 cM–*D1S2844* genetic interval containing nicastrin. However, these results do not preclude the existence of risk alleles in other data sets and/or in non-coding regulatory sequences of nicastrin in families within our data set. Furthermore, these data do not abrogate a role for wild-type nicastrin in the pathogenesis of abnormal βAPP processing in Alzheimer's disease due to environmental and other genetic causes. Indeed, because manipulation of an exposed domain of nicastrin has significant effects on βAPP processing, nicastrin is potentially a tractable target for therapeutic modulation of Aβ production in patients with Alzheimer's disease and related disorders. □

Methods

Purification of the nicastrin protein

Membrane proteins were purified from HEK293 cells stably overexpressing moderate levels of wild-type human PS1, extracted with digitonin and fractionated on a 10–40% glycerol gradient containing 0.5% digitonin as described[3,40]. The peak PS1-containing fractions (which contain ~0.5 g of membrane proteins) were pooled and incubated overnight with Protein A/G agarose coupled with either an affinity-purified PS1 NTF antibody (antibody 1142; P. E. Fraser, unpublished data) or a control IgG purified from pre-immune rabbit serum. After washing six times with buffer (1% digitonin, 0.5% CHAPS, 20 mM HEPES pH 7.2, 100 mM KCl, 10 mM $CaCl_2$, 5 mM $MgCl_2$ and a protease inhibitor cocktail), isolated protein complexes were eluted with 0.1 M glycine-HCl pH 3.0, separated by Tris-glycine SDS–PAGE gels, and stained with silver stain or Coomassie blue stain. Individual protein bands were cut out and analysed with SPE-CE-tandem mass spectroscopy[22]. Protein bands were first digested in-gel with trypsin; the digested peptides were extracted and concentrated in a speed vacuum; the peptides were separated by solid-phase extraction capillary electrophoresis and analysed by on-line tandem mass spectrometry. High quality MS/MS spectra were selected and used for the protein sequence and translated nucleotide sequence database searches.

Nicastrin cDNAs

Full-length human, murine and *Drosophila melanogaster* nicastrin cDNAs were obtained

using oligonucleotides designed from partial cDNA/expressed sequence tag sequences in public databases (http://www.ncbi.nlm.nih.gov) to screen appropriate cDNA libraries, for 5′ RACE and/or for polymerase chain reaction with reverse transcription (RT–PCR) experiments. Chromosomal locations and genetic map positions of the murine and human nicastrins were obtained from public genetic and transcriptional maps (http://www.ncbi.nlm.nih.gov). A nicastrin expression construct was generated by inserting human nicastrin cDNA in-frame with the V5 epitope of pcDNA6 at the C terminus of nicastrin.

Cell lines

HEK293 cells were transiently or stably transfected with either V5-tagged nicastrin or V5–LacZ or empty plasmid (controls). We have noticed that the level of nicastrin in cells stably expressing nicastrin constructs tends to fall over time, suggesting that overexpression of nicastrin may be slightly toxic. We also used previously characterized HEK293 cell lines expressing PS1/PS2 and/or βAPP or SP-C99-βAPP to evaluate the interaction of nicastrin with PS1, PS2 and βAPP[3,4,14,41,42].

Biochemical methods

Brain tissue, cultured cells and partially purified cell membranes were lysed with 1% digitonin lysis buffer or with 1% NP40, and the protein extracts were subjected to gradient fraction, immunoprecipitation or direct western blotting as described[3].

Antibodies

V5-epitope-tagged nicastrin was detected using anti-V5 (Invitrogen, CA). Polyclonal rabbit anti-nicastrin anti-sera were raised against residues 290–406 of human nicastrin fused to glutathione *S*-transferase (anti-N-NCT), or against a peptide containing residues 691–709 (anti-C-NCT). Antibodies included anti-PS1-NCT (Ab14, S. Gandy; 1142); or anti-PS1-CTF (N. Brindle); anti-PS2 (DT2, P. Davies); anti-FL-βAPP and C-terminal α- and β-secretase derivatives (369, S. Gandy).

Aβ assays

$A\beta_{40}$ and $A\beta_{42}$ levels were measured as described[43] by ELISA using 6–20-h conditioned media collected from HEK293 cells stably expressing both βAPP ($\beta APP_{Swedish}$ or $\beta APP_{wild\text{-}type}$) and either nicastrin (wild type or one of its mutants) or a control sequence (LacZ or empty vector). The Aβ levels in cells transfected with a control sequence (LacZ or empty vector) were set at 1.0 and the Aβ levels in test samples were then normalized to this value. Transformed (square root transformation) data were compared by a priori planned pairwise Student's *t*-test[44].

RNA interference

Sense and antisense RNA were transcribed *in vitro* from PCR products amplified from the *C. elegans* nicastrin cDNA phage yk477b8 (Y. Kohara). After annealing equal quantities of sense and antisense products, we injected the dsRNA into L4 stage animals. Injected animals were transferred to fresh plates daily and the progeny scored at least 36 h after injection for the embryonic lethal phenotype and for 4–5 days after injection for other phenotypes. The penetrance of the embryonic lethal phenotype ranged from 75 to 100% of the total brood.

Received 24 March; accepted 21 July 2000.

1. Sherrington, R. *et al.* Cloning of a gene bearing missense mutations in early onset familial Alzheimer's disease. *Nature* **375,** 754–760 (1995).
2. Rogaev, E. I. *et al.* Familial Alzheimer's disease in kindreds with missense mutations in a novel gene on chromosome 1 related to the Alzheimer's disease type 3 gene. *Nature* **376,** 775–778 (1995).
3. Yu, G. *et al.* The presenilin 1 protein is a component of a high molecular weight intracellular complex that contains β-catenin. *J. Biol. Chem.* **273,** 16470–16475 (1998).
4. Nishimura, M. *et al.* Presenilin mutations dominantly modulate *β*-catenin trafficking. *Nature Med.* **5,** 164–169 (1999).
5. De Strooper, B. *et al.* Post-translational modification, subcellular localization and membrane orientation of the Alzheimer's Disease associated Presenilins. *J. Biol. Chem* **272,** 3590–3598 (1997).
6. De Strooper, B. *et al.* Deficiency of presenilin 1 inhibits the normal cleavage of amyloid precursor protein. *Nature* **391,** 387–390 (1998).
7. Ye, Y., Lukinova, N. & Fortini, M. E. Neurogenic phenotypes and altered Notch processing in *Drosophila* presenilin mutants. *Nature* **398,** 525–529 (1999).
8. Struhl, G. & Greenwald, I. Presenilin is required for activity and nuclear access of Notch in *Drosophila*. *Nature* **398,** 522–525 (1999).
9. De Strooper, B. *et al.* A presenilin dependent gamma-secretase-like protease mediates release of Notch intracellular domain. *Nature* **398,** 518–522 (1999).
10. Song, W. *et al.* Proteolytic release and nuclear translocation of Notch-1 are induced by presenilin-1 and impaired by pathogenic presenilin-1 mutations. *Proc. Natl Acad. Sci. USA* **96,** 6959–6963 (1999).
11. Katayama, T. *et al.* Presenilin-1 mutations downregulate the signalling pathway of the unfolded-protein response. *Nature Cell Biol.* **1,** 479–485 (1999).
12. Niwa, M., Sidrauski, C., Kaufman, R. J. & Walter, P. A role for presenilin-1 in nuclear accumulation of Ire1 fragments amd induction of the mammalian Unfolded Protein Response. *Cell* **99,** 691–702 (1999).
13. Scheuner, D. *et al.* Secreted amyloid-*β* protein similar to that in the senile plaques of Alzheimer Disease is increased *in vivo* by presenilin 1 and 2 and APP mutations linked to FAD. *Nature Med.* **2,** 864–870 (1996).
14. Citron, M. *et al.* Mutant presenilins of Alzheimer's Disease increase production of 42 residue amyloid *β*-protein in both transfected cells and transgenic mice. *Nature Med.* **3,** 67–72 (1997).
15. Wolfe, M. S. *et al.* Two transmembrane aspartates in presenilin 1 required for presenilin endoproteolysis and gamma-secretase activity. *Nature* **398,** 513–517 (1999).
16. Li, Y. M. *et al.* Photoactivated gamma-secretase inhibitors directed to the active site covalently label presenilin 1. *Nature* **405,** 689–694 (2000).
17. Thinakaran, G. *et al.* Evidence that levels of presenilins (PS1 and PS2) are coordinately regulated by competition for limiting cellular factors. *J. Biol. Chem.* **272,** 28415–28422 (1997).
18. Li, Y.-M. *et al.* Presenilin 1 is linked with gamma-secretase activity in the detergent solubilized state. *Proc. Natl Acad. Sci. USA* **97,** 6138–6143 (2000).
19. Yu, G. Mutation of conserved aspartates affect maturation of both aspartate-mutant and endogenous presenilin 1 and presenilin 2 Complexes. *J. Biol. Chem.* (in the press).
20. Feldman, R. G., Chandler, K. A., Levy, L. L. & Glaser, G. H. Familial Alzheimer's Disease. *Neurology* **13,** 811–824 (1963).
21. Foncin, J.-F. *et al.* Démence présénile d'Alzheimer transmise dans une famille étendue. *Rev. Neurol. (Paris)* **141,** 194–202 (1985).
22. Figeys, D., Ducret, A., Yates, J. R. & Aebersold, R. Protein identification by solid phase microextraction-capillary zone electrophoresis-microelectrospray-tandem mass spectroscopy. *Nature Biotech.* **14,** 1579–1583 (1996).
23. Zhou, J. *et al.* Presenilin 1 interacts with a novel member of the armadillo family. *NeuroReport* **8,** 2085–2090 (1997).
24. Levesque, G. *et al.* Presenilins interact with armadillo proteins including neural specific plakophilin related protein and beta-catenin. *J. Neurochem.* **72,** 999–1008 (1999).
25. Kehoe, P. *et al.* A full genome scan for late onset Alzheimer's Disease. *Hum. Mol. Genet.* **8,** 237–245 (1999).
26. Zubenko, G. S., Hughes, H. B., Stiffler, J. S., Hurtt, M. R. & Kaplan, B. B. A genome survey for novel Alzheimer disease risk loci: results at 10 cM resolution. *Genomics* **50,** 121–128 (1998).
27. Preiss, J. R., Schnabel, H. & Schnabel, R. The glp-1 locus and cellular interactions in early *C. elegans* embryos. *Cell* **51,** 601–611 (1987).
28. Li, X. & Greenwald, I. HOP-1, A *Caenorhabditis elegans* presenilin, appears to be functionally redundant with SEL12 presenilin and to facilitate LIN-12 and GLP-1 signalling. *Proc. Natl Acad. Sci. USA* **94,** 12204–12209 (1998).
29. Westlund, B., Barry, D., Clover, R., Basson, M. & Johnson, C. D. Reverse genetic analysis of *C. elegans* presenilins reveals redundant but unequal roles for sel-12 and hop-1 in Notch-pathway signaling. *Proc. Natl Acad. Sci. USA* **96,** 2497–2502 (1999).
30. Goutte, C., Hepler, W., Mickey, K. M. & Priess, J. R. aph-2 encodes a novel extracellular protein required for GLP-1-mediated signaling. *Development* **127,** 2481–2492 (2000).
31. Hussain, I. *et al.* Identification of a novel aspartic protease (Asp 2) as beta-secretase. *Mol. Cell Neurosci.* **14,** 419–427 (1999).
32. Sinha, S. *et al.* Purification and cloning of amyloid precursor protein beta-secretase from human brain. *Nature* **402,** 537–540 (1999).
33. Vassar, R. *et al.* Beta-secretase cleavage of Alzheimer's Amyloid precursor protein by the transmembrane aspartic protease BACE. *Science* **286,** 735–741 (1999).
34. Yan, R. *et al.* Membrane-anchored aspartyl protease with Alzheimer's Disease beta-secretase activity. *Nature* **402,** 533–537 (1999).
35. Selkoe, D. J. Normal and abnormal biology of *β*-Amyloid Precursor Protein. *Ann. Rev. Neurosci.* **17,** 489–517 (1994).
36. Xia, W., Zhang, J., Perez, R., Koo, E. H. & Selkoe, D. J. Interaction between amyloid precursor protein and presenilins in mammalian cells: implications for the pathogenesis of Alzheimer Disease. *Proc. Natl Acad. Sci. USA* **94,** 8208–8213 (1997).
37. Ray, W. J. *et al.* Evidence for a physical interaction between presenilin and Notch. *Proc. Natl Acad. Sci. USA* **96,** 3263–3268 (1999).
38. Thinakaran, G. *et al.* Stable association of the presenilin derivatives and absence of presenilin interactions with APP. *Neurobiol. Disease* **4,** 438–453 (1998).
39. Capell, A. *et al.* The proteolytic fragments of the Alzheimer's Disease associated presenilin-1 form heterodimers and occur as a 100–150 kDa molecular mass complex. *J. Biol. Chem.* **273,** 3205–3211 (1998).
40. Hay, J. C., Chao, D. S., Kuo, C. S. & Scheller, R. H. Protein interaction regulating vesicle transport between the endoplasmic reticulum and Golgi apparatus in mammalian cells. *Cell* **89,** 149–158 (1997).
41. Citron, M. *et al.* Additive effects of PS1 and APP mutations on secretion of the 42-residue amyloid beta-protein. *Neurobiol. Dis.* **5,** 107–116 (1998).
42. Chen, F. Proteolytic derivative of Amyloid Precursor Protein accumulate in restricted and unpredicted intracellular compartments in the absence of functional presenilin 1 expression. *J. Biol. Chem.* (in the press).
43. Zhang, L., Song, L. & Parker, E. M. Calpain inhibitor 1 increases beta-Amyloid peptide production by inhibiting the degradation of the substrate of gamma-secretase. *J. Biol. Chem.* **274,** 8966–8972 (1999).
44. Howell, D. C. *Statistical Methods for Psychology* (Duxbury Press, California, 1992).

Supplementary information is available on *Nature*'s World-Wide Web site (http://www.nature.com) or as paper copy from the London editorial office of *Nature*.

Acknowledgements

This work was supported by grants from the Medical Research Council of Canada, Alzheimer Association of Ontario, Howard Hughes Medical Research Foundation, Scottish Rite Charitable Foundation, Helen B. Hunter Fellowship (G.Y.), Peterborough Burgess Fellowship (E.A.R.), NIH (R.A. and L.F.); the National Institute of Aging Alzheimer Disease Center Grant (L.F.), University of Toronto Department of Medicine Postgraduate Fellowship (M.N.) and Japan Society for the Promotion of Science (T.K.). The PS2 D366A construct was from C. Haass. We thank R. Feldman and J.-F. Foncin for their work on the Nicastro pedigrees, and C. Goutte and J. R. Preiss for sharing pre-publication data.

Correspondence and requests for materials should be addressed to P.St G.-H. (e-mail: p.hyslop@utoronto.ca).

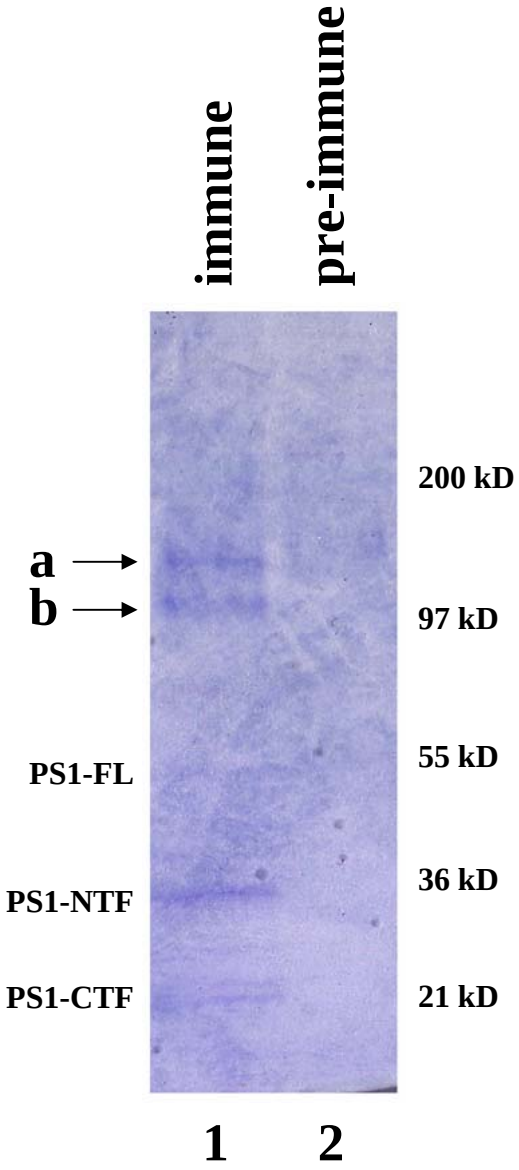

Supplemental fig 1

Isolation of the presenilin-1 complex. Coomassie Blue stained electrophoretic gel of immunoprecipitation products from HEK293 cells overexpressing wild-type human PS1 immunoprecipitated either with anti-PS1-NTF antibody 1142 (“immune”) or pre-immune serum. Band “a” contained nicastrin and some a-catenin; band “b” contained b-catenin; PS1 holoprotein, PS1-NTF and PS1-CTF containing bands are depicted accordingly.

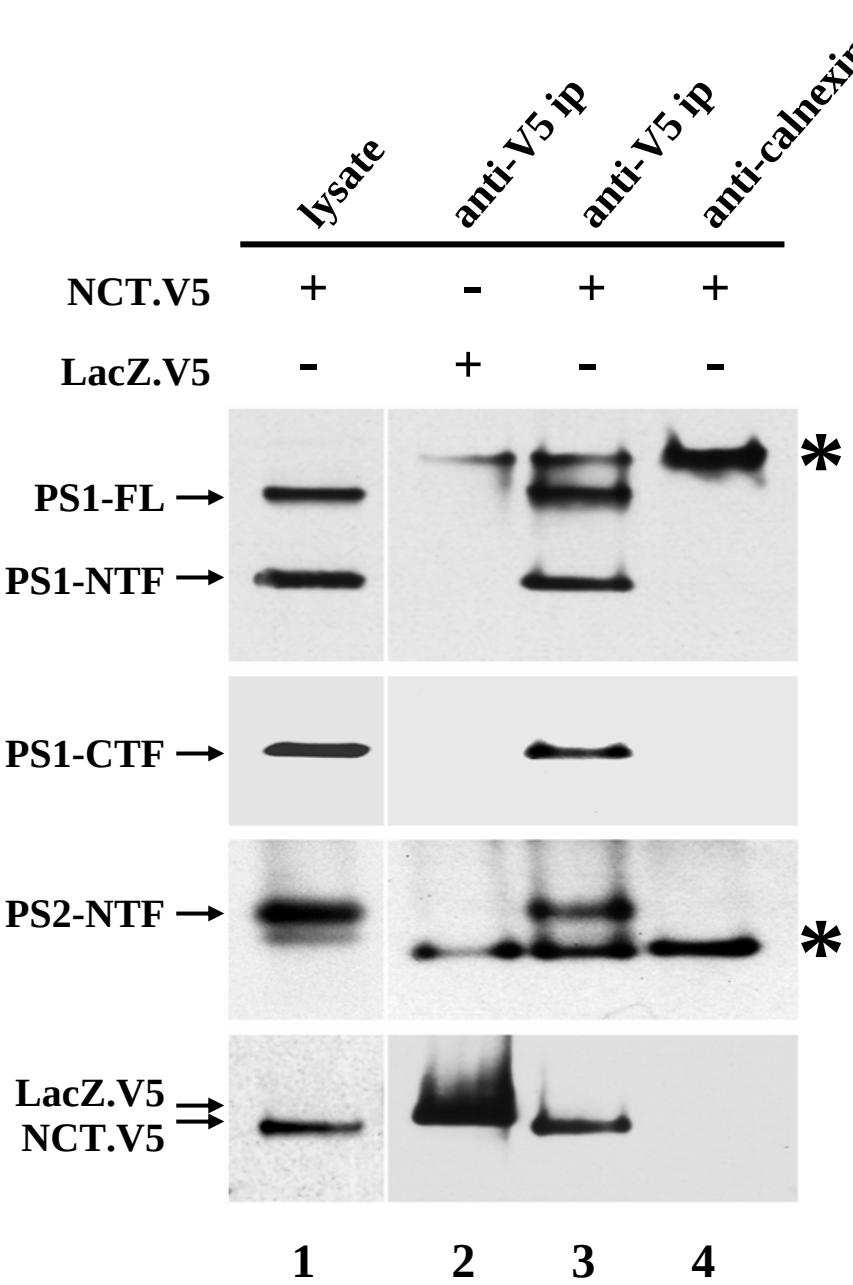

Supplemental fig 2
PS1 and PS2 form complexes with nicastrin in HEK293 cells overexpressing human PS1 and nicastrin. Anti-PS1/2 (top three panels) and anti-V5 (lower panel) western blots of anti-V5 immunoprecipitation products show that PS1 holoprotein, NTF, CTF and PS2-NTF co-immunoprecipitate with V5-tagged nicastrin (lane 3), but not V5-tagged beta-galactosidase (lane 2) or calnexin (lane 4). Lane 1 represent ~30% of the starting lysates utilized for immunoprecipitation. Asterisk represents IgG.

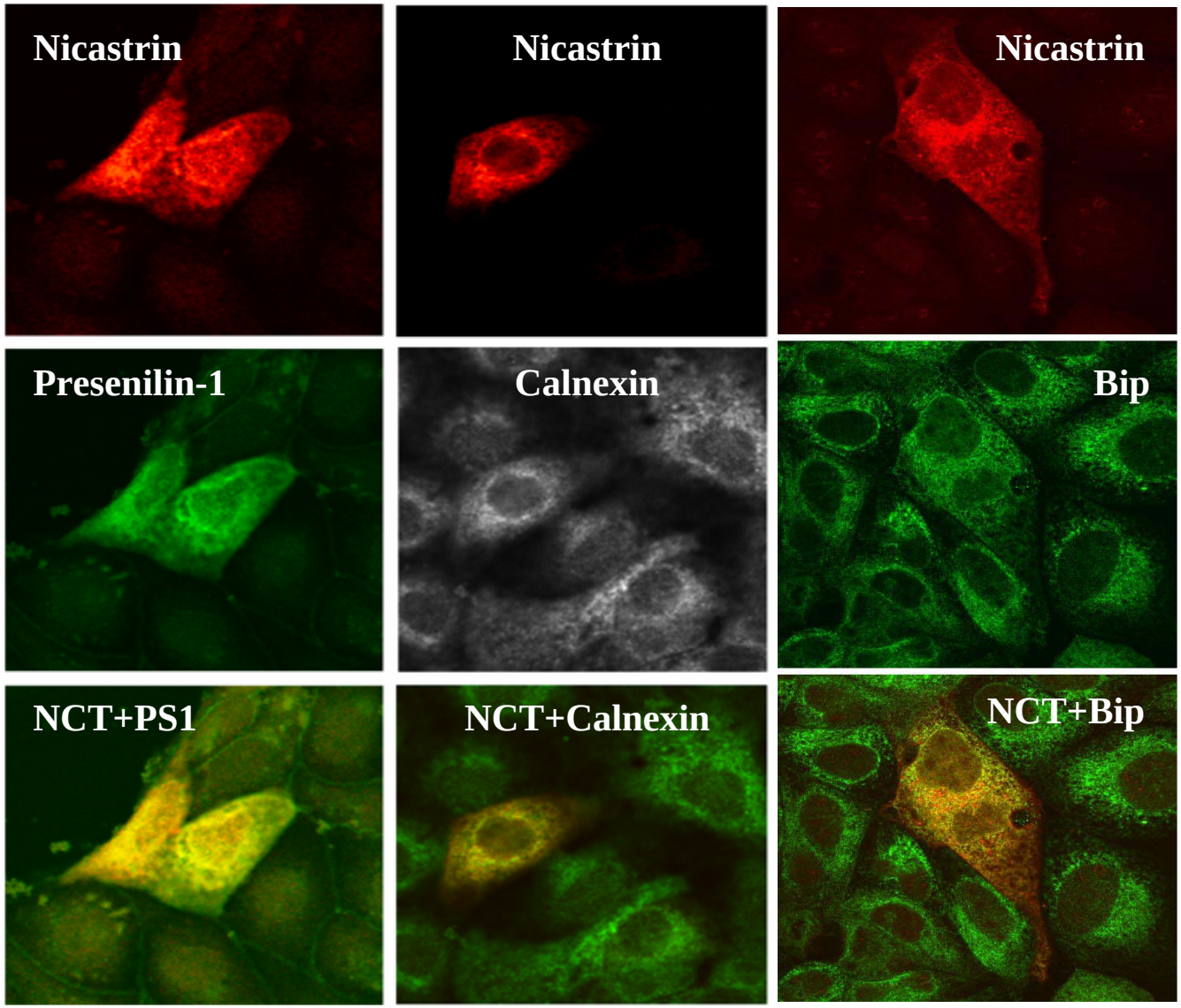

Supplemental fig 3

Colocalization of nicastrin and presenilin-1 in ER. Confocal images of MDCK cells transiently transfected with human nicastrin and PS1, and immuno-stained with anti-nicastrin (red) and either anti-PS1 or anti-calnexin or anti-Bip (green) antibodies, following Triton-X100 permeabilization. Yellow color indicates colocalization of NCT with PS1 or ER-markers calnexin and Bip.

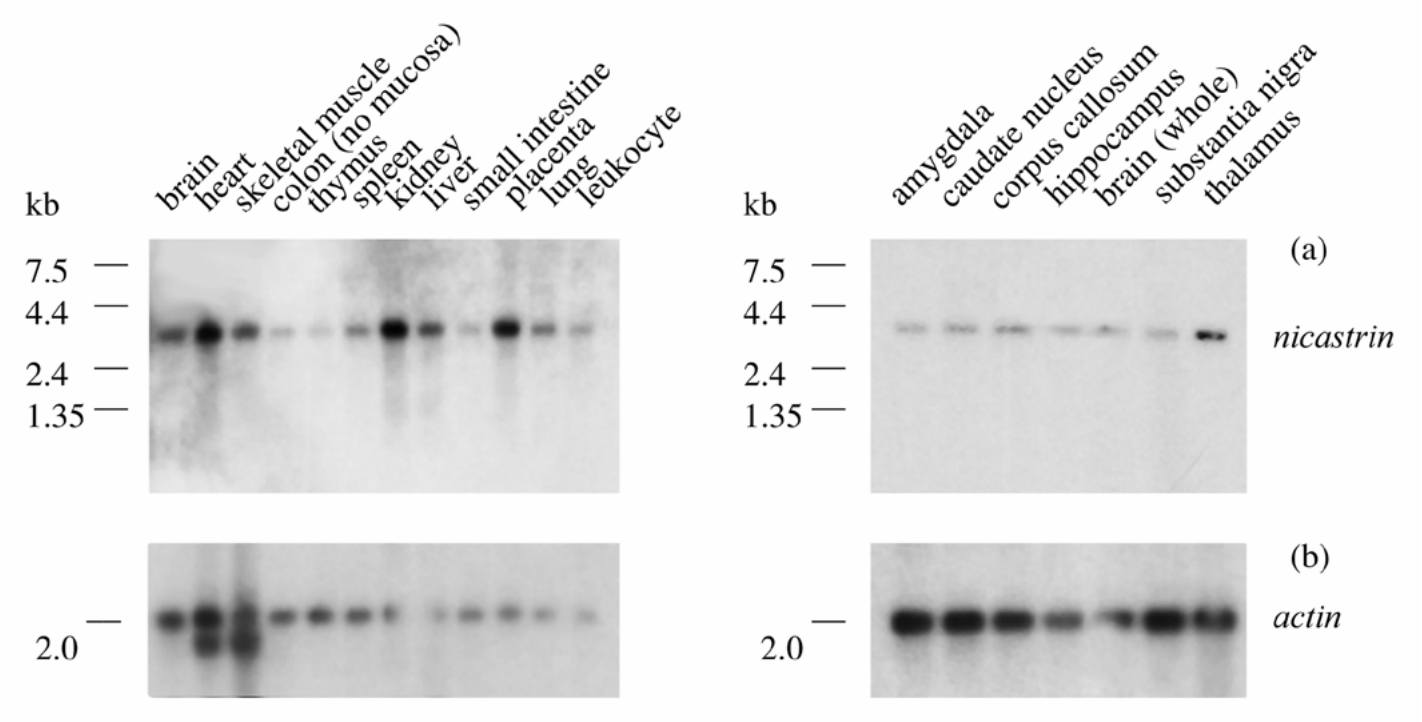

Supplemental fig 4

mRNA expression patterns of nicastrin. The nicastrin gene probe was hybridized to northern blots (Clontech, California) containing mRNA from various regions of human brain and from other tissues. The blots were also rehybridized using the actin probe as a control for mRNA loading.

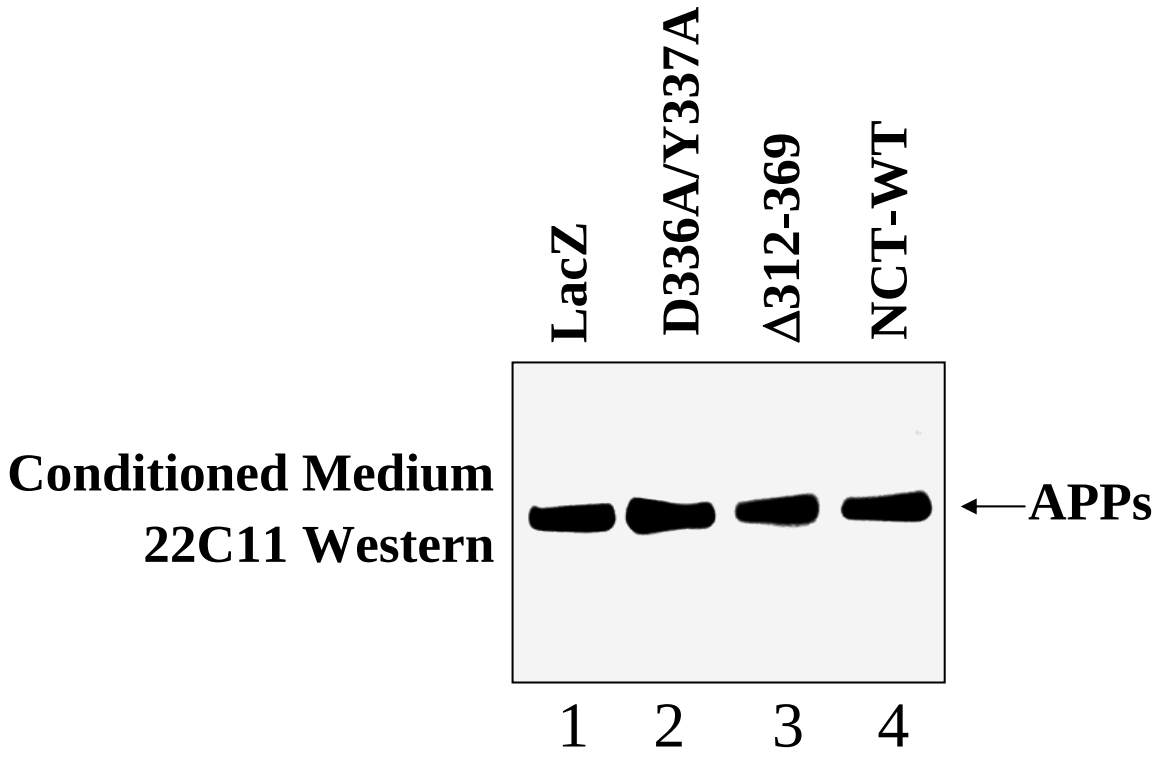

Supplemental fig 5

Secreted APPs level in conditioned media from different nicastrin cell lines. Anti-APP (22C11) western blot of conditioned media from HEK293 cells overexpressing APPsw and either wild-type nicastrin (lane 4), or D312-369 mutant nicastrin (lane 3), or D336A/Y337A mutant nicastrin (lane 2), or LacZ (lane 1).

Table 1

Transfection Cell Type	Normalised $A\beta_{42}$	Normalised $A\beta_{40}$	$A\beta_{42}/A\beta_{40}$ Ratio
Mock (LacZ/empty vector)	1.0	1.0	1.0
wild type nicastrin	1.00 ± 0.09	1.01 ± 0.08	0.99 ± 0.06
D336A/Y337A	2.73 ± 0.33 ($p < 0.001$)	1.61 ± 0.11 ($p = 0.001$)	1.63 ± 0.09 ($p < 0.001$)
$nicastrin_{\Delta 312\text{-}369}$	0.05 ± 0.04 ($p < 0.001$)	0.31 ± 0.06 ($p < 0.001$)	0.09 ± 0.05 ($p < 0.001$)
$nicastrin_{\Delta 312\text{-}340}$	0.33 ± 0.04 ($p = 0.001$)	0.55 ± 0.04 ($p = 0.001$)	0.59 ± 0.06 ($p = 0.001$)

Supplemental Table 1
Table of mean ± standard error of mean normalized Ab levels in supernatants from stable HEK293 cell lines over-expressing wild type or mutant nicastrin cDNAs, LacZ, or empty vector.